SUPPORTING INFORMATION

SI Materials and Methods

Cell Culture and Reagents. MCF-7, T47D, T47D-kBluc, HCC-1500, ZR-75-1, MCF10A, MDA MB-231, CAOV-3, OVCAR-3, IGROV-1, ES2, ECC-1, HeLa, PC-3, DU145, H1793, A549, MEF, and HepG2 cells were obtained from the ATCC. Dr. E. Wilson provided HeLa-AR13 cells, Dr. K. Korach provided BG-1/MCF-7 cells, Dr. B.H. Park provided $MCF10A_{ER\ IN9}$ cells, Dr. R. Schiff provided BT-474 cells, and E. Alarid provided MCF7ERαHA cells. Prior to experiments, to deplete cells of estrogens in the serum and medium, ERα positive cell lines were maintained for 4 days in medium supplemented with phenol red-free charcoal-dextran (CD) treated serum.

Chemical Libraries and Screening. The small molecule libraries screened were: The ~150,000 small molecule Chembridge MicroFormat small molecule library, the ~10,000 small molecule University of Illinois Marvel library developed by Drs. K. Putt and P. Hergenrother (1), and the ~2,000 small molecule NCI diversity set obtained from NIH. High throughput screening for small molecule inhibitors of endogenous E_2-ERα induced expression of the stably transfected $(ERE)_3$-luciferase reporter in T47D-KBluc cells, was carried out using the assay we recently described (2).

Cell Proliferation Assays: Cells were resuspended in the following media and plated in 96 well plates at the indicated densities: MCF-7 (10% CD-calf, 1,000 cells); MCF7ERαHA (10% CD-calf, 1,000); T47D (10% CD-calf, 2,000); T47D- kBluc (10% CD-FBS, 1,000); HCC-1500 (10% CD-FBS, 1,000); BT-474 (10% CD-calf, 2,000); ZR-75-1 (10% CD-calf 2,000); $MCF10A_{ER\ IN9}$ (2% CD-FBS, 1,000); MCF10A (2% CD-FBS, 1,000); MDA MB-231 (10% FBS, 1,000); BG-1/MCF-7 (5% FBS, 250); CaOV-3 (10% CD-CALF, 2,000); OVCAR-3 (10% CD-FBS, 2,000); IGROV-1 (10% FBS, 1,000); ES2 (10% FBS, 1,000); ECC-1 (5% CD-FBS, 1,000); Ishikawa (10% CD-calf, 2,000); HeLa (10% FBS, 1,000); PC-3 (10% CD-FBS, 1,000); DU145 (10% FBS, 1,000); 201T (10% FBS, 2,000); 273T (10% FBS, 1,000); H1793 (5% FBS, 2,000); A549 (10% FBS, 1,000); HepG2 (10% CD-FBS, 1,000), MEF (10% FBS, 2,000). The medium was replaced with treatment medium the following day, and plates were incubated at 37° C in 5% CO_2 for 4 days except for BT-474, BG-1/MCF-7 and Ishikawa which were incubated for 6 days and ZR-75-1 cells which were incubated for 7 days. Treatment solutions were replaced every two days. Cell number was determined from MTS assays using CellTiter 96 Aqueous One Solution Reagent (Promega). For each cell line, cell number was calculated from a standard curve of the number of plated cells versus A_{490}.

ATP Measurements*:* To measure ATP levels, cells were lysed and ATP luminescence levels were measured using an ATPlite Luminesence Assay kit (PerkinElmer, MA). ATP released from cells was quantified from a standard curve of ATP standards versus luminescence.

Luciferase Assays. Reporter gene assays were carried out, as previously described (2, 3). Briefly, cells were switched to 10% CD-FBS for four days prior to experiments, and plated at a density of 50,000 cells/well in 24-well plates. The medium was replaced the next day with medium containing the test compounds, with or without hormone, incubated for 24 hours and luciferase assays were performed using Bright Glow reagent (Promega, WI).

qRT-PCR. RNA was extracted using a QiaShredder kit (Qiagen) for cell homogenization, and purified with the RNAeasy mini-kit (Qiagen, CA). cDNA was prepared from 0.5 μg of RNA by reverse transcription using a DyNAmo cDNA synthesis kit (Finnzymes, Finland). Quantitative PCR assays were performed on samples from 3 independent sets of cells (biological triplicate). Reactions contained 10 ng of cDNA and 50 nM forward and reverse primers in 15 μl and were carried out using Power SYBR Green PCR Mastermix (Applied Biosystems).

The fold change in expression of each gene was calculated using the $\Delta\Delta C_t$ method with the ribosomal protein 36B4 used as the internal control, as described previously (2, 4, 5).

Chromatin Immunoprecipitation. Chromatin Immunoprecipitation. MCF-7 cells were stripped of estrogens for 3 days in 5% CD-FBS. Cells were pretreated with 1 μM BHPI or DMSO (0.1%) as a control for 105 minutes, and then were treated with either 10 nM E_2 or an ethanol-vehicle control (0.1%) for 45 minutes. ChIP was carried out essentially, as previously described (3).

Transfections. siRNA knockdowns were performed using DharmaFECT1 Transfection Reagent and 100 nM ON-TARGETplus non-targeting pool or SMARTpools for ERα (ESR1), PLCγ (PLCG1), PERK (EIF2AK3), or pan-IP_3R (Dharmacon). The pan-IP_3R SmartPool consisted of three individual SmartPools, each at 33 nM, directed against each isoform of the IP_3R (ITPR1, ITPR2, and ITPR3). To knockdown ERα, $MCF10A_{ER\ IN9}$ cells were treated for 16 hours with either human ERα SMARTpool (ESR1) siRNA or Non-targeting Control Pool siRNA. Cells were treated with transfection complex for 16 hours, and medium was replaced with DMEM/F12, supplemented with 2% CD-FBS. ERα knockdown at the mRNA and protein level was assessed every 24 hours following transfection. The effects of BHPI on protein synthesis following ERα knockdown were assessed 3-days post-knockdown by treating cells with either 0.1% DMSO loading control or 100 nM BHPI for the indicated times and protein synthesis was then assessed by measuring ^{35}S-Methionine incorporation. Knockdowns of PERK, IP_3R, and PLCγ were performed by maintaining MCF-7 cells in MEM containing 5% CD-FBS for 4 days prior to plating cells in serum-free MEM. Cells were treated with transfection complexes for 16 hours and medium was replaced with MEM, supplemented with 10% CD-calf serum. The effects of BHPI on protein synthesis or calcium signaling were assessed 3-days post-knockdown. The eIF2α S51A plasmid was a gift from Dr. David Ron (Addgene plasmid # 21808). ECC-1 cells (4×10^3) were transfected with either 0.2 μg of eIF2α S51A plasmid DNA or empty expression vector. Transfections were performed using Lipofectamine 3000, according to manufacture instructions. Cells were treated with 100 nM BHPI 30 hours after transfection, and protein synthesis was evaluated by measuring ^{35}S-Methionine incorporation.

Immunoblotting. Western blotting was carried out as previously described (2, 4, 6). The following antibodies were used: ERα [6F11] antibody (Biocare Medical, CA), Phospho-eIF2α (Ser51) (#3398; Cell Signaling Technology), eIF2α (#5324; Cell Signaling Technologies, MA), Phospho-eEF2 (#2331; Cell Signaling Technology, MA), eEF2 (#2332; Cell Signaling Technology, MA), Phospho-p44/42 MAPK (#4370; Cell Signaling Technology, MA), p44/42 MAPK (#4695; Cell Signaling Technology, MA), Phospho-PERK (#3179; Cell Signaling Technology, MA), PERK (#5683; Cell Signaling Technology, MA), ATF6α (Imgenex, CA), Phospho-AMPKα (#2535; Cell Signaling Technology, MA), AMPKα (#2603; Cell Signaling Technology, MA), Phospho-AMPKβ1 (#4181; Cell Signaling Technology, MA), AMPKβ1/2 (#4150, Cell Signaling Technology, MA), Phospho-Acetyl-CoA Carboxylase (#3661; Cell Signaling Technology, MA), Acetyl-CoA Carboxylate (#3676; Cell Signaling Technology, MA), Phospho-IP_3R (#8548; Cell Signaling Technology, MA), IP_3R (#8568; Cell Signaling Technology, MA), Pan-IP_3R (sc-28613; Santa Cruz, CA), Phospho-PLCγ (#2821; Cell Signaling Technology, MA), PLCγ (#5690; Cell Signaling Technology, MA), BiP (#3177; Cell Signaling Technology, MA), $p58^{IPK}$ (#2940; Cell Signaling Technology, MA), laminin A/C (Santa Cruz, CA), β-Actin (Sigma, MO), and α-Tubulin (Sigma, MO). Bound antibodies were detected using horseradish peroxidase-conjugated secondary antibodies and chemiluminescent immunodetection with an ECL Detection Kit (GE Healthcare, NJ), and were visualized using a PhosphorImager.

Nuclear-cytoplasmic Distribution of ERα. MCF-7 cells were pre-treated with 1 μM BHPI or DMSO (0.1%) for 30 minutes, followed by 2 hours with or without E_2. Nuclear and cytoplasmic extraction was carried out on ~6 million cells/treatment using a NE-PER Nuclear and Cytoplasmic Extraction Reagents (ThermoScientific). Lamin A/C and α-Tubulin, were used as nuclear and cytoplasmic markers, respectively.

Protein Synthesis. Protein synthesis rates were evaluated by measuring incorporation of ^{35}S-Methionine into newly synthesized protein. Cells were plated at a density of 10,000 cells/well in 96-well plates. Cells were incubated for 30 minutes with 3 μCi of ^{35}S methionine (PerkinElmer, MA) per well at 37° C. Cells were washed two times with PBS, and lysed using 30 μL of RIPA buffer. Cell lysates were collected in microfuge tubes and clarified by centrifugation at 13,000 x g for 10 min at 4° C. Samples were normalized to total protein, and the appropriate volume of sample was spotted onto Whatman 540 filter paper discs and immersed in cold 10% TCA. The filters were washed once in 10% TCA and 3 times in 5% TCA and air dried. Trapped protein was then solubilized and the filters were counted.

Calcium Imaging. Cytoplasmic Ca^{2+} concentrations were measured using the calcium-sensitive dye, Fluo-4 AM. The cells were grown on 35 mm-fluorodish cell culture plates (#FD35-100, World Precision Instruments) for two days prior to imaging experiments. The cells were loaded with 5 μM Fluo-4 AM (Life Technologies, CA) in HEPES-based buffer (140 mM NaCl, 4.7 mM KCl, 1.13 mM $MgCl_2$, 10 mM HEPES, 10 mM Glucose, pH = 7.4) for 30 minutes at 37° C before measurement of intracellular calcium. The cells were washed three times with HEPES buffer to remove extracellular Fluo4-AM dye and incubated with either 2 mM $CaCl_2$ or 0 mM $CaCl_2$ for 10 minutes to complete de-esterification of the dye. Confocal images were obtained for one minute to determine basal fluorescence intensity, and then the appropriate treatment was added. Confocal images were captured using a Zeiss LSM 700 confocal system, Plan-Four 20X objective (N.A. = 0.8) and scanned at a resolution of 512x512 pixels (780ms/min). To minimize photo-bleaching and photo-toxicity of samples, the laser power was reduced to 7%. For fluorescence measurements, the cells were excited at 488 nm, and the emission was collected at 525 nm. Images were acquired and analyzed with AxioVision and Zen software (Zeiss). Calcium traces were generated by normalizing fluorescence to basal fluorescence intensity. Data presented as mean ± standard error (n = 10 individual cells).

Protease Sensitivity Assays: ERα LBD (N304-S554) containing an N-terminal 6-His tag, was expressed and purified as described previously (7), and stored in Tris-HCl buffer (50 mM Tris-HCl pH 8.0, 10% glycerol, 2 mM DTT, 1 mM EDTA, and 1 mM Na_3VO_4). Purified ERα LBD protein (10 μg) was incubated with 500 nM E_2 for 20 min at 37° C. Samples were then treated with either DMSO vehicle, BHPI (1 μM) or inactive Compound 8 (1 μM) and incubated for 20 min at 37° C. For partial protease cleavage, the binding mixture was added with/without protease K at a concentration of 7.5 ng protease K per μg protein. After incubation for 10 min at 22° C, the digestions were terminated by addition of SDS sample buffer buffer. The denatured samples were analyzed on a 15% SDS-PAGE gel and visualized by coomassie blue staining.

Intrinsic Fluorescence Spectroscopy: The stock solution of full-length ERα was diluted to 400 nM in a Tris-Buffer (50 mM Tris/HCl pH8.0, 150 mM KCl, 2 mM DTT, 1 mM EDTA, and 10% glycerol). The intrinsic fluorescence measurements were carried out in a 10 mm quartz cuvette using a Varian Cary Eclipse Fluorescence Spectrophotometer. The excitation and emission slits were set at 5 nm. Tryptophan fluorescence was measured using an excitation wavelength of 295 nm. Emission spectra were collected from 310-380 nm. All spectra were collected at 37° C. E_2 (500 nM), BHPI (500 nM), or inactive compound 88 (500 nM) was added and incubated at 37°C for 10 min, and then the ERα emission spectra were recorded. All the spectra were corrected for baseline in the absence of E_2.

Colony Formation Assays: Assays to assess anchorage-independent cell proliferation in soft agar were carried out as previously described (3). Each treatment condition was evaluated on five independent sets of cells. Culture medium was changed every 3 days. Colonies were visible after 2 weeks, and total colonies were counted at Day 21 using a dissecting microscope. Photographs of colonies were taken using a Zeiss AxioImager2 imaging system at 5X magnification.

Mouse xenograft. All experiments were approved by the Institutional Animal Care Committee (IACUC) of the University of Illinois at Urbana-Champaign. The MCF-7 cell mouse xenograft model has been described previously (8). At least 12 animals, with 2-4 tumors per animal, were required per experimental group to

maintain significant statistical power to detect >25% difference in tumor growth rates. Briefly, estrogen pellets (1 mg:19 mg estrogen:cholesterol) were implanted into 60 athymic female OVX mice, which were 7 weeks of age. Three days after E_2 pellet implantation 1 million MCF-7, human breast cancer cells per site in matrigel were subcutaneously injected at 2 sites in each flank for a total of 4 potential tumors per mouse. When the average tumor size reached 17.6 mm^2 (4.7 by 4.7 mm), E_2 pellets were removed and a lower dose of E_2 in sealed silastic tubing (1:31 estrogen:cholesterol, 3 mg total weight) was implanted in the same site. When the average tumor size reached 23.5 mm^2 (5.5 by 5.5 mm), mice were divided into 4 groups with tumor size normalized: E_2 group, no treatment control (NC) group, B_10 group and B_1/B_15 group. E_2 silastic tubes in the NC group were removed, while E_2 silastic tubes in the E2, B_10, and B_1/B_15 groups were retained. The E_2 and NC group received intraperitoneal injection every other day with 10 ml/kg vehicle (2% DMSO, 10% Tween-20, and 88% PBS). The B_10 group received 10 mg/kg BHPI by intraperitoneal injection every other day. The B_1/B_15 group received 1 mg/kg BHPI by intraperitoneal injection every other day for 14 days. Since this extremely low BHPI dose had no effect, (average tumor cross-sectional area ~45 mm^2) they then received 15 mg/kg BHPI every day for another 10 days. Food intake and body weight were measured every 4 days and food intake is presented as grams/day. Tumors were measured every 4 days with a caliper. Tumor cross sectional area was calculated as (a/2)*(b/2)*3.14, where a and b were the measured diameters of each tumor. On termination of the experiments mice were euthanized and the tumors were excised and weighed. 2 of 60 mice were removed during the course of the study, one that failed to form tumors and the other due to unrelated illness. No tumors were excluded from analysis, and blinding was not performed.

IP_3 Quantitation. MCF-7 cells were incubated for 10 minutes in 100 nM E_2, 10 μM BHPI or vehicle. Intracellular IP_3 levels were determined by extracting the cells, and determining IP_3 levels in an assay based on competition with radiolabeled IP_3 for binding to a recombinant fragment of IP_3R containing the IP_3 binding site. Unlabeled IP_3 provided a standard for the competition assays. $1.5x10^6$ MCF-7 cells were incubated with ice-cold 1 M trichloroacetic acid (TCA) containing 1 mM EDTA on ice for 15 min. After centrifugation, the supernatant was collected and incubated for 15 min. at room temperature. The TCA solution was removed by adding two volumes of 1,1,2-Trichloro-1,2,2-trifluoroethane (TCTFE)-trioctylamine solution. The TCTFE-solution was prepared by mixing 3:1 (v/v) of TCTFE and trioctylamine (Sigma). Unlabeled IP_3, labeled, IP_3 and the unlabeled IP_3R fragment were from Perkin Elmer (Waltham, MA) and were used largely according to the supplier's directions. Briefly, unlabeled IP_3 standards or cell extracts were incubated with the working receptor/tracer solution at 1:4 (v/v) for 1 hr. at 4^o C. The samples were sedimented by centrifugation at 2,000xg for 20 min and the supernatant was discarded. The pellet was suspended in 0.15 M NaOH. After 15 min. at room temperature, the samples were mixed with 5 ml of Pico-Fluor Plus scintillation fluid (Perkin Elmer, Watham, MA) and radioactivity determined by scintillation counting. IP_3 levels in biological samples were calculated from the standard curve generated using a range of unlabeled IP_3 concentrations.

EDC Dendrimer. The EDC dendrimer was prepared and used as previously described (9).

SI Figures

A

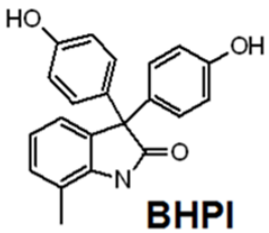

BHPI

B

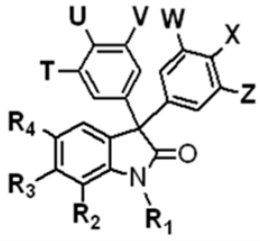

Comp.	R_1	R_2	R_3	R_4	T	U	V	W	X	Z	IC_{50} (μM)
BHPI	-H	-Me	-H	-H	-H	-OH	-H	-H	-OH	-H	.015
1	-H	-Me	-Cl	-H	-H	-OH	-H	-H	-OH	-H	.015
2	-H	-H	-H	-H	-H	-OH	-H	-H	-OH	-H	.150
3	-H	-H	-H	-Br	-H	-OH	-H	-H	-OH	-H	.300
4	-H	-H	-H	-H	-F	-OH	-H	-F	-OH	-H	.300
5	-Me	-H	-H	-H	-H	-OH	-H	-H	-OH	-H	.750
6	-Me	-Me	-H	-Br	-H	-OH	-H	-H	-OH	-H	1.5
7	-H	-H	-H	-H	-Me	-OH	-H	-H	-OH	-Me	7.5
8	-H	-H	-H	-H	-H	-OH	-Me	-H	-OH	-Me	7.5
9	-H	-Me	-H	-Me	-H	-OH	-Me	-H	-OH	-Me	>10

Fig. S1. BHPI and structurally related compounds selectively inhibit estrogen-dependent cell proliferation. (*A*) Structure of BHPI (3,3-bis(4-hydroxyphenyl)-7-methyl-1,3,dihydro-2Hindol-2-one). (*B*) Inhibition of the proliferation of T47D cells by BHPI and by structurally related compounds (n = 6).

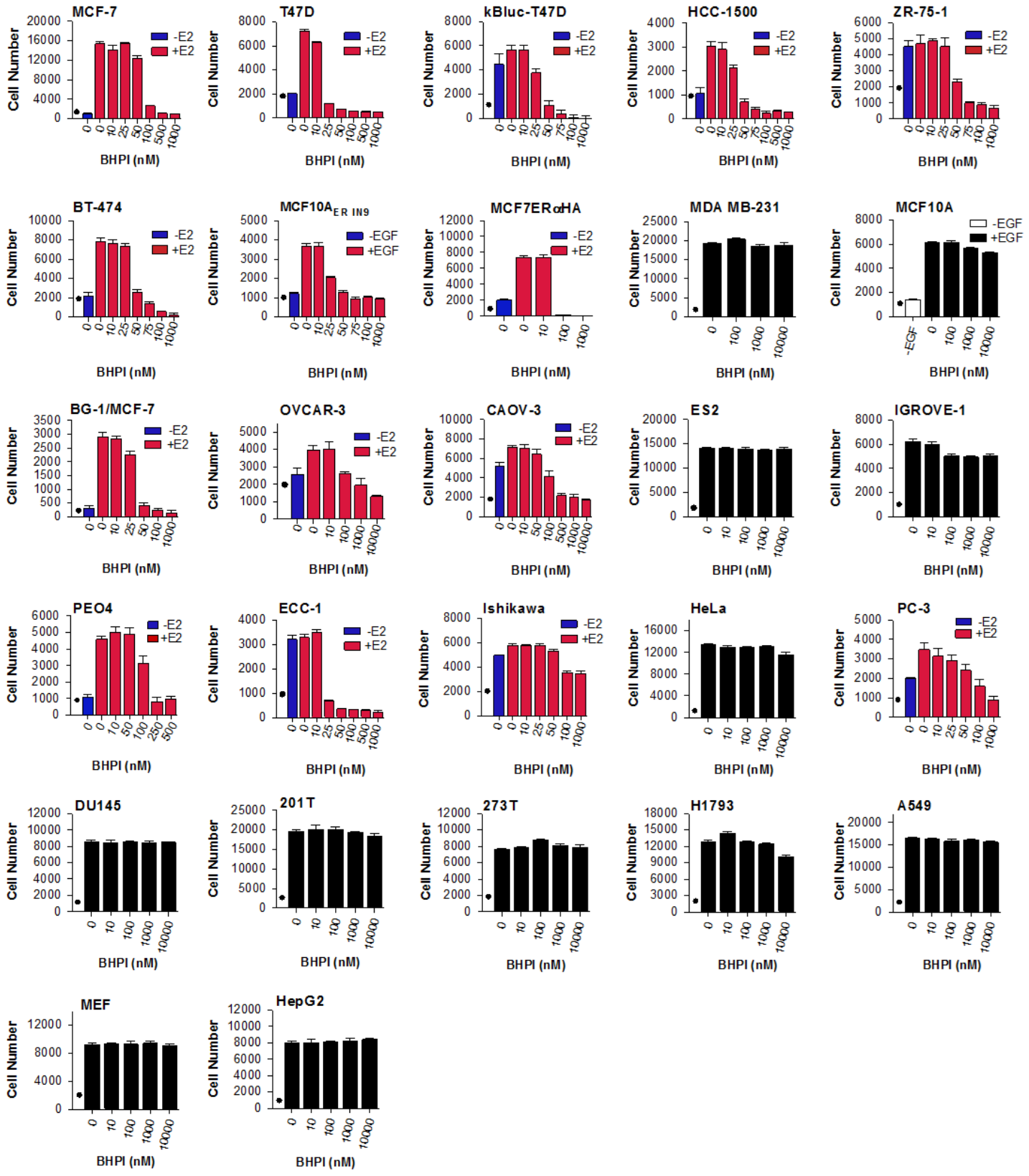

Fig. S2. BHPI selectively inhibits cell proliferation in ERα positive cancer cells. Effects of BHPI on cell proliferation in 15 ERα positive (colored bars) and 12 ERα negative (black bars) cell lines. Cell lines are grouped by tissue of origin (breast, ovary, cervix, prostate, lung and liver). "•" on each graph denotes the number of cells at the start of the experiment. Most cell proliferation studies were for 3 or 4 days in 10 nM E_2. Since we recently found that our BG-1 cells are genetically identical to MCF-7 cells, that data is presented as BG-1/MCF-7. Data is the mean ± SEM (n = 6).

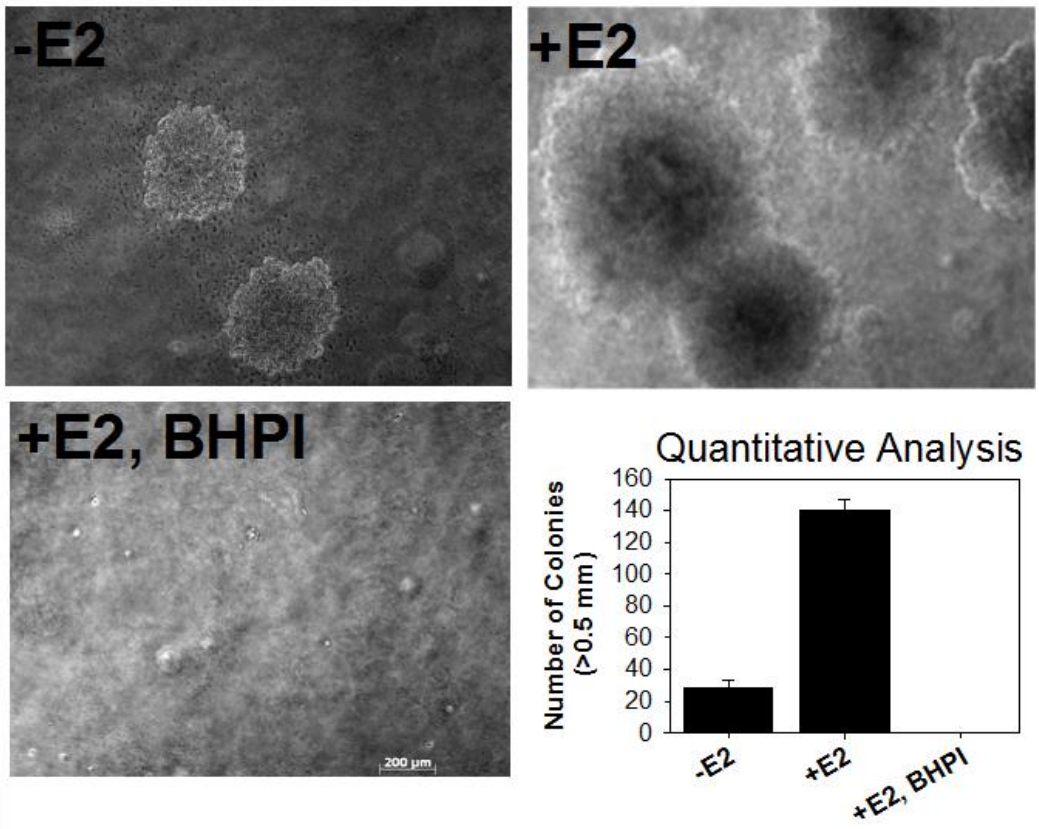

Fig. S3. BHPI inhibits anchorage-independent growth of MCF-7 cells in soft agar. 5,000 MCF-7 cells were plated into top agar. Cells were treated with medium containing DMSO (vehicle) and either, 10 nM E_2 (+E2) or Ethanol (vehicle) (-E2), or 1 μM BHPI and 10 nM E_2 (+E2, BHPI). Medium was changed every 3 days. After 21 days, colonies were counted and photographed at 5x magnification. For each treatment, the bar graph represents the average of the total number colonies per well with a diameter >0.5 mm. Data is the mean ± SEM (n = 6).

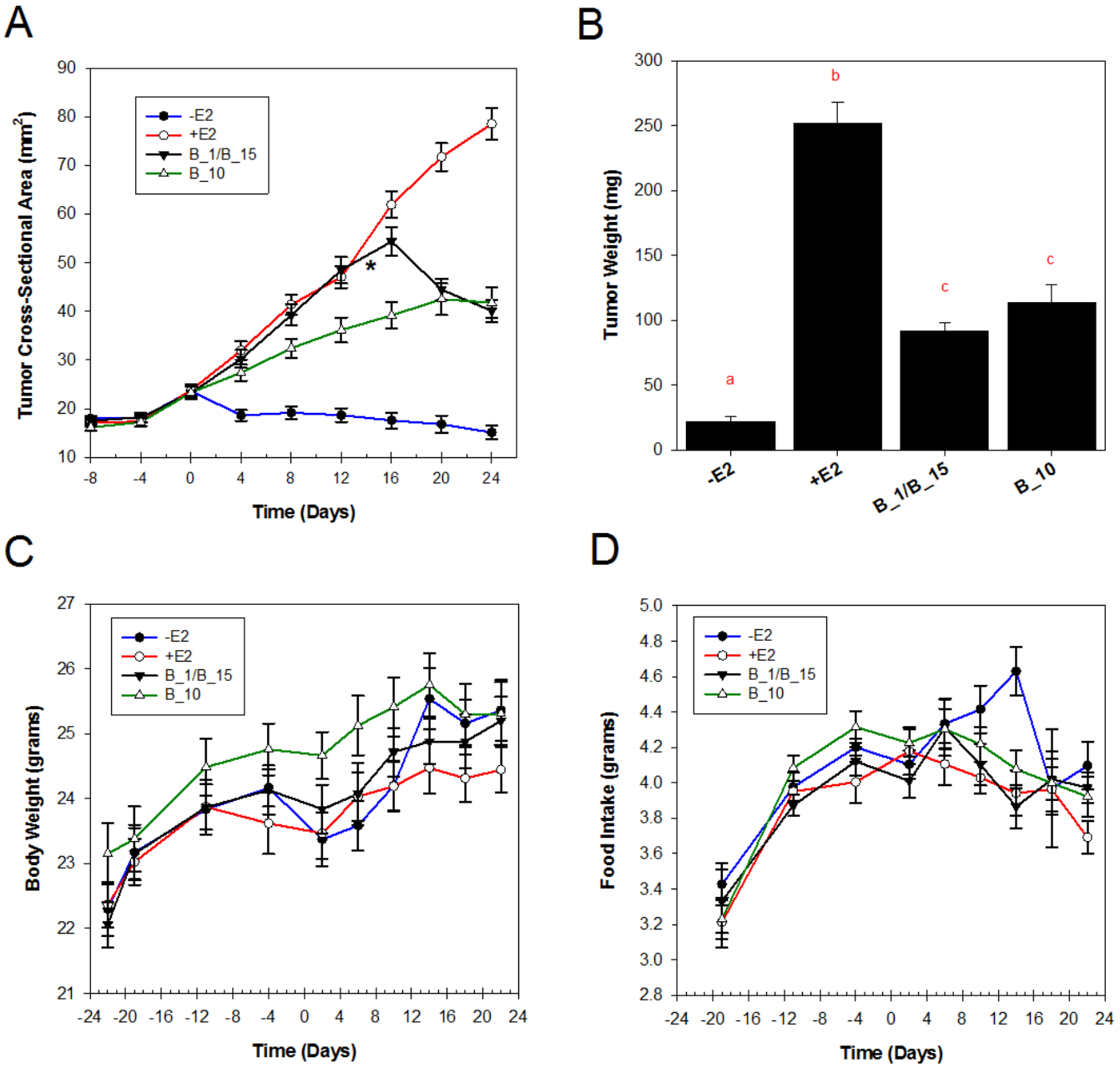

Fig. S4. BHPI inhibits tumor growth in a mouse xenograft model of breast cancer and is not toxic. (*A*) MCF-7 tumor growth in athymic mice was monitored every 4 days by measuring tumor diameter with a caliper. The E2 and –E2 group received vehicle injection, while the B_10 group was injected with 10 mg/kg BHPI every other day. The B_1/B_15 group received the extremely low dose of 1 mg/kg BHPI every other day for 14 days. This very low dose of BHPI had no effect on tumor growth. They then received 15 mg/kg BHPI every day until the end of the study (* denotes change in dosage). Tumor size was represented as tumor cross sectional area (mm^2). Each tumor was analyzed individually, and data are expressed as mean ± SEM (n = 52). (*B*) Mice were sacrificed and tumor weights were recorded. Data is expressed as mean ± SEM (n = 52) and analyzed using one way ANOVA with post hoc Fisher's LSD test. Different letters indicate significant differences between groups ($p < 0.05$). (*C*) Mouse body weight was measured every 4 days after initiation of drug injection. Data is expressed as mean ± SEM (n = 13). (*D*) Mouse food intake was measured every 4 days after initiation of drug injection. Data expressed as mean ± SEM (n = 13). BHPI treatment had no effect on body weight or food intake and was therefore not overtly toxic.

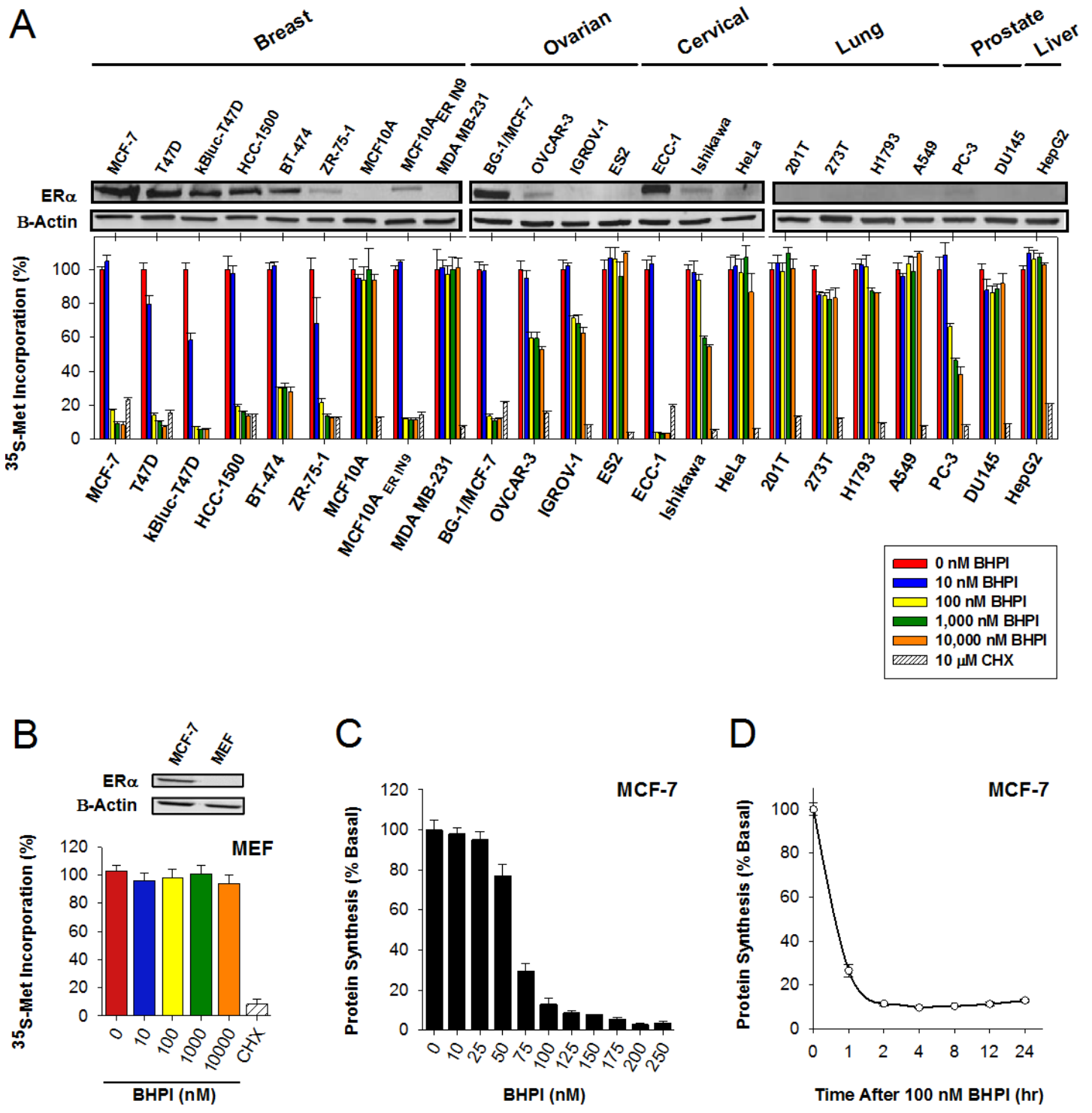

Fig. S5. BHPI selectively inhibits protein synthesis in ERα positive cells in 26 cells lines (PEO4 data shown in Figure 3*A* and MCF7ERαHA data shown in Figure 3*E*). (*A*) Comparison of ERα protein levels and the effects of BHPI treatment on protein synthesis in 23 cell lines. The number of samples was too large to run on a single gel and the data is from 3 identically processed gels. (*B*) Effects of BHPI on protein synthesis in ERα$^-$ Mouse Embryo Fibroblast (MEF) cells. Incorporation with no added BHPI was set to 100%. In general, protein synthesis in cells expressing moderate or high levels of ERα was robustly inhibited by 100 nM BHPI (yellow bars), while 10,000 nM BHPI (orange bars), the highest concentration tested, had very little or no effect on protein synthesis in ERα negative cells. Cells expressing low levels of ERα, more typical of non-transformed ERα containing cells, such as PC-3 prostate cancer cells, were much less sensitive to BHPI inhibition of protein synthesis. Western blot of ERα protein levels in MEF cells. (*C*) Dose-response curve, which shows the

effects of increasing concentrations of BHPI on protein synthesis in MCF-7 cells following 24-hour treatment. The narrow dose-response curve is consistent with either activation of the autoactivated kinase PERK, or with a threshold level of calcium required for PERK activation (*D*) Time course showing the effect of 100 nM BHPI on protein synthesis in MCF-7 cells. Data is the mean ± SEM (n = 4).

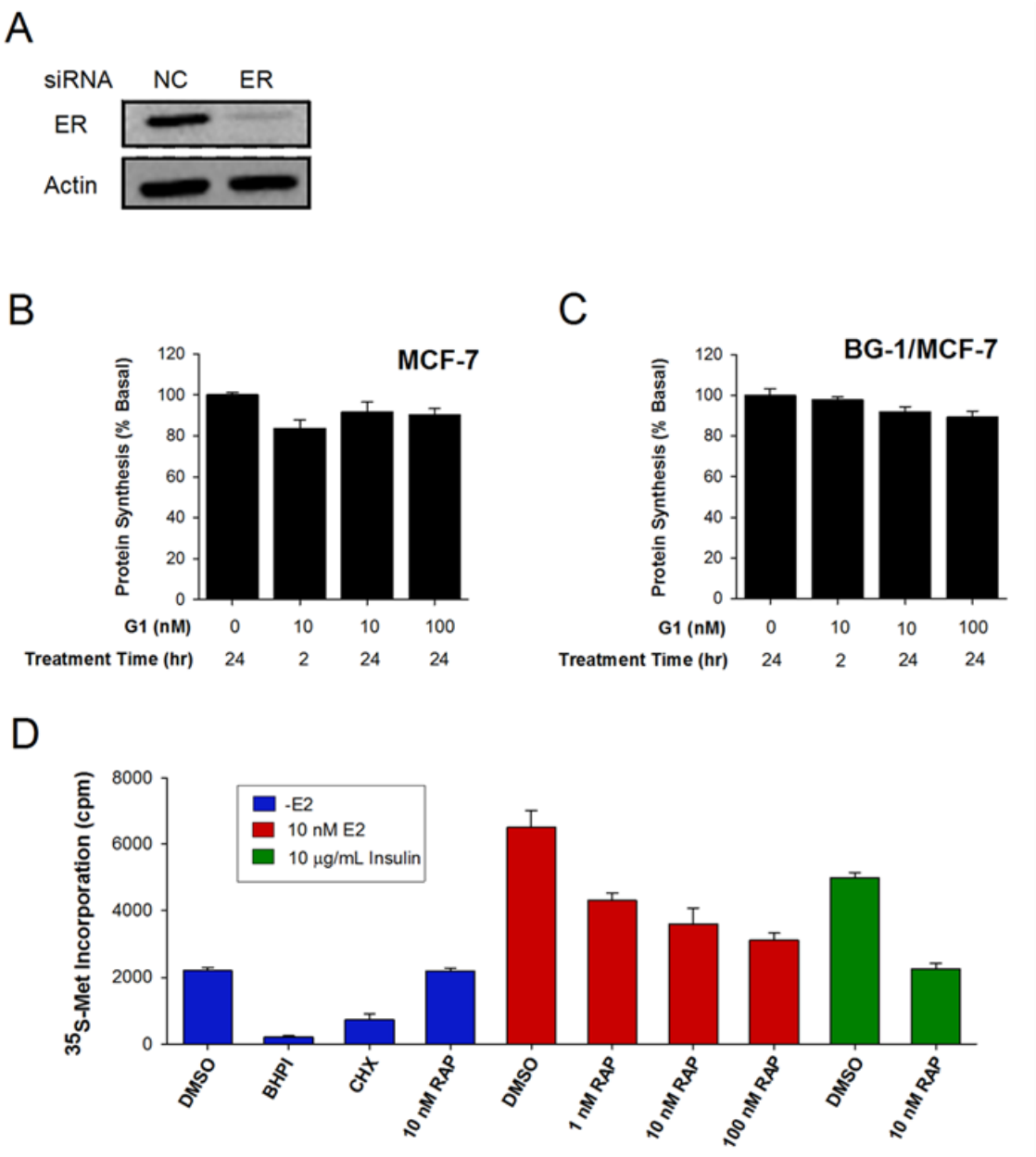

Fig. S6. Activation of the estrogen binding protein, GPR30, or inhibition of mTOR, have minimal effects on protein synthesis**.** (*A*) Western blot analysis of ERα levels after treatment of MCF-7 cells with either 100 nM non-coding SmartPool siRNA or 100 nM SmartPool ERα siRNA. Effects of the GPR30 activator, G1, on (*B*) MCF-7 and (*C*) BG-1/MCF-7 cells. Cells were plated at 10,000 cells/well, the indicated concentrations of G1 (0-100 nM) were added for the times indicated, and ^{35}S-Methionine incorporation was used to assess rates of protein synthesis. Protein synthesis with no added G1 was set to 100%. (*D*) The effects of rapamycin (RAP) on protein synthesis in MCF-7 cells in the absence of growth factors (blue bars), or in the presence of 10 nM E2 (red bars) or 10 µg/ml Insulin (green bars). Inhibition of mTORC1 with rapamycin blocks insulin-dependent increases in protein synthesis (green bars) and substantially blocks estrogen-dependent increases in protein synthesis (red bars). In contrast, BHPI and cycloheximide (CHX) treatment elicit near-quantitative inhibition of protein synthesis, far below baseline levels of protein synthesis (blue bars). Data is mean ± SEM (n = 4).

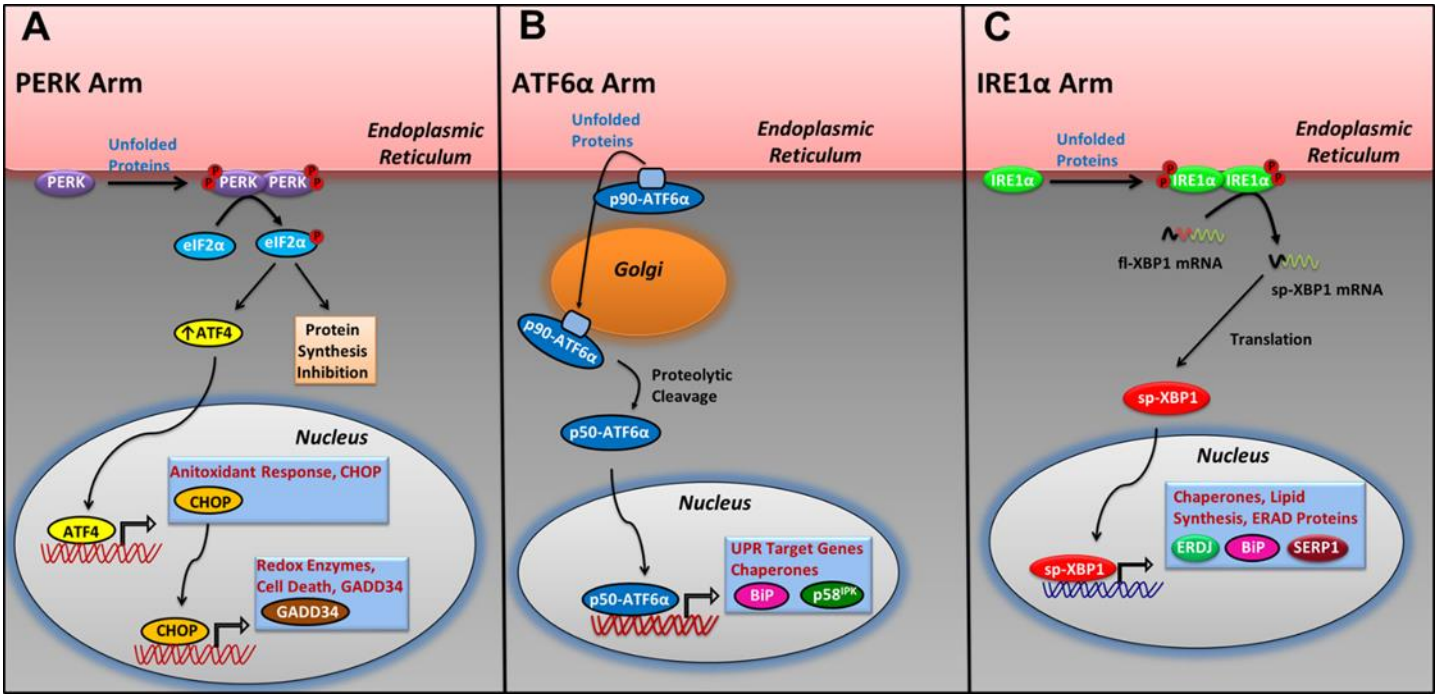

Fig. S7. Endoplasmic reticulum (EnR) stress activates the three arms of the UPR. (*A*) EnR stress induces the oligomerization and phospho-activation of the transmembrane kinase PERK. P-PERK phosphorylates eukaryotic initiation factor 2α (eIF2α), leading to inhibition of protein synthesis and a reduction in the endoplasmic reticulum protein folding load (10, 11). Reduced protein synthesis increases levels of the transcription factor, ATF4. ATF4 induces the transcription factor CHOP, which induces GADD34 and several pro-apoptotic genes. (*B*) EnR stress promotes the translocation of the transmembrane protein, p90-ATF6α, from the EnR to the Golgi Apparatus, where it encounters proteases that liberate the N-terminal fragment of ATF6α (p50-ATF6). p50-ATF6 increases the protein-folding capacity of the EnR by inducing EnR-resident chaperones, including BiP and GRP94 (10-12). (*C*) EnR stress induces the oligomerization and phospho-activation of the transmembrane protein, IRE1α (10, 11, 13). Activated IRE1α removes an intron from full-length XBP1 (fl-XBP1) mRNA, producing spliced (sp)-XBP1 mRNA, which is subsequently translated into sp-XBP1 protein (sp-XBP1). sp-XBP1 increases the protein-folding capacity of the EnR and turnover of misfolded proteins by inducing EnR resident-chaperone protein genes (BiP, HEDJ, SERP1), EnR-associated degradation (ERAD) genes and alters mRNA decay and translation (10, 11).

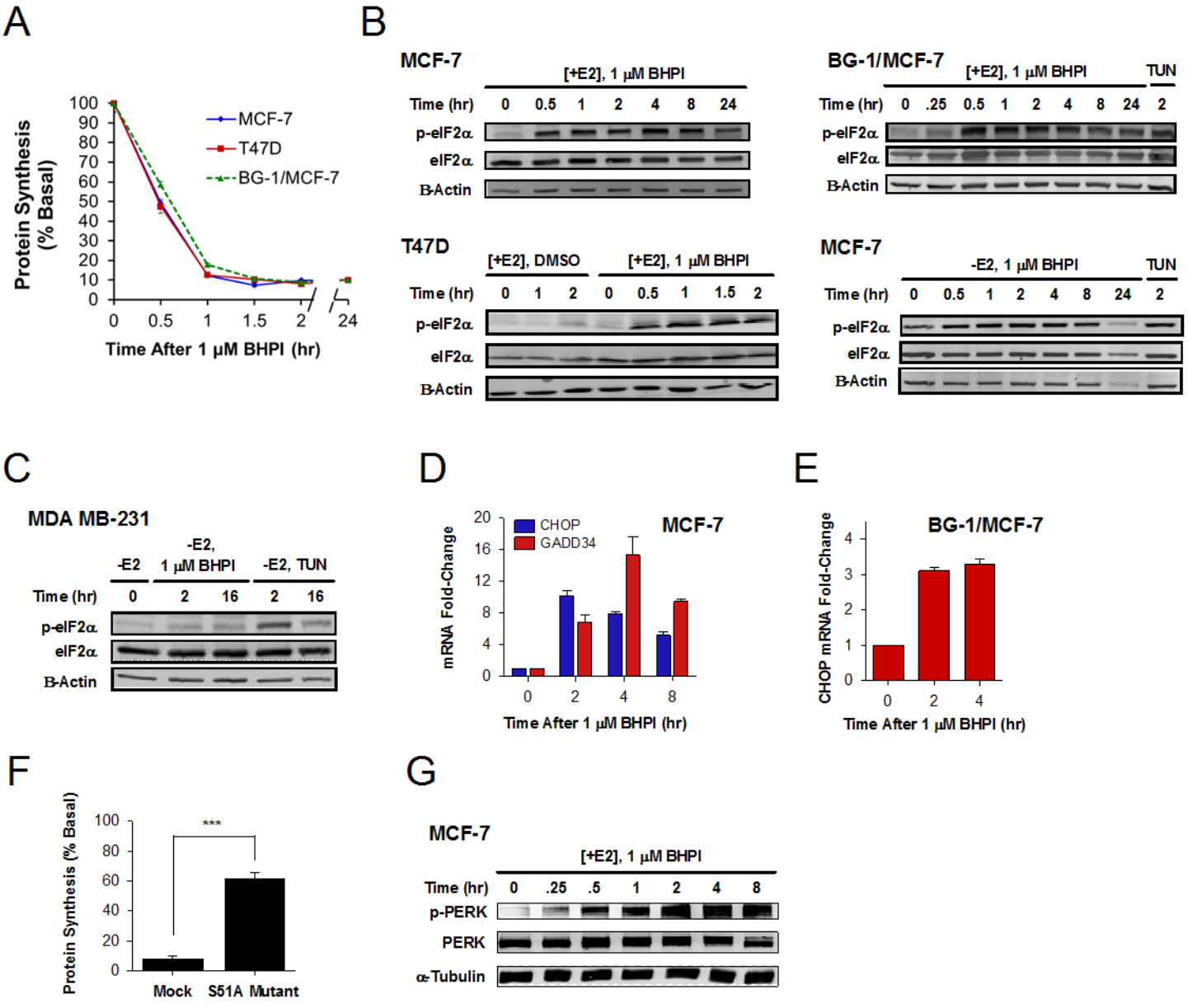

Fig. S8. In ERα positive cell lines, BHPI rapidly inhibits protein synthesis by activating the PERK arm of the UPR. (*A*) Time course of BHPI inhibition of protein synthesis. ERα positive MCF-7, T47D, and BG-1/MCF-7 cells were incubated for the indicated times with 1 μM BHPI. Set to 100% was incorporation of ^{35}S-methionine into protein at time = 0. Data is mean ± SEM (n = 4). At 30 min. with BHPI, ^{35}S-methionine incorporated into protein was reduced by ~50%. (*B*) In the presence [+E2], BHPI increases p-eIF2α (Ser-51) in ERα$^+$ MCF-7, BG-1/MCF-7, and T47D cells. In the absence of estrogen (-E2), BHPI increases eIF2α phosphorylation in ERα$^+$ MCF-7 cells. (*C*) BHPI does not increase p-eIF2α in ERα negative MDA MB-231 cells. Since the UPR activator Tunicamycin (TUN) increased p-eIF2α in these cells, the absence of BHPI induced phosphorylation of eIF2α in the MDA-MB-231 cells was not due to the inability of UPR activation to induce eIF2α phosphorylation. (*D*) Induction of CHOP and GADD34 mRNA in MCF-7 cells following treatment with 1 μM BHPI, as determined by qRT-PCR. (*E*) Induction of CHOP mRNA in BG-1/MCF-7 cells following treatment with 1 μM BHPI. Increased levels of ATF4 induce the transcription factor, CHOP, which then induces GADD34. Increased phosphorylation of eIF2α results in translational upregulation of the transcription factor, ATF4. ATF4 contains short, inhibitory upstream open reading frames (uORFs), which normally inhibit translation of ATF4

mRNA (10). Under conditions of reduced eIF2α availability, the inhibitory uORFs are skipped, allowing ATF4 translation. (*F*) Effects of 100 nM BHPI on protein synthesis following transfection of ECC-1 endometrial cells with either a dominant-negative eIF2αS51A mutant or empty vector. Data is the mean ± SEM (n = 4). *** $p < 0.001$. (*G*) Time course of phosphorylation of PERK (Thr-980) and total PERK protein levels following treatment with BHPI in MCF-7 cells. PERK-Thr^{980} phosphorylation serves as a marker of PERK activation.

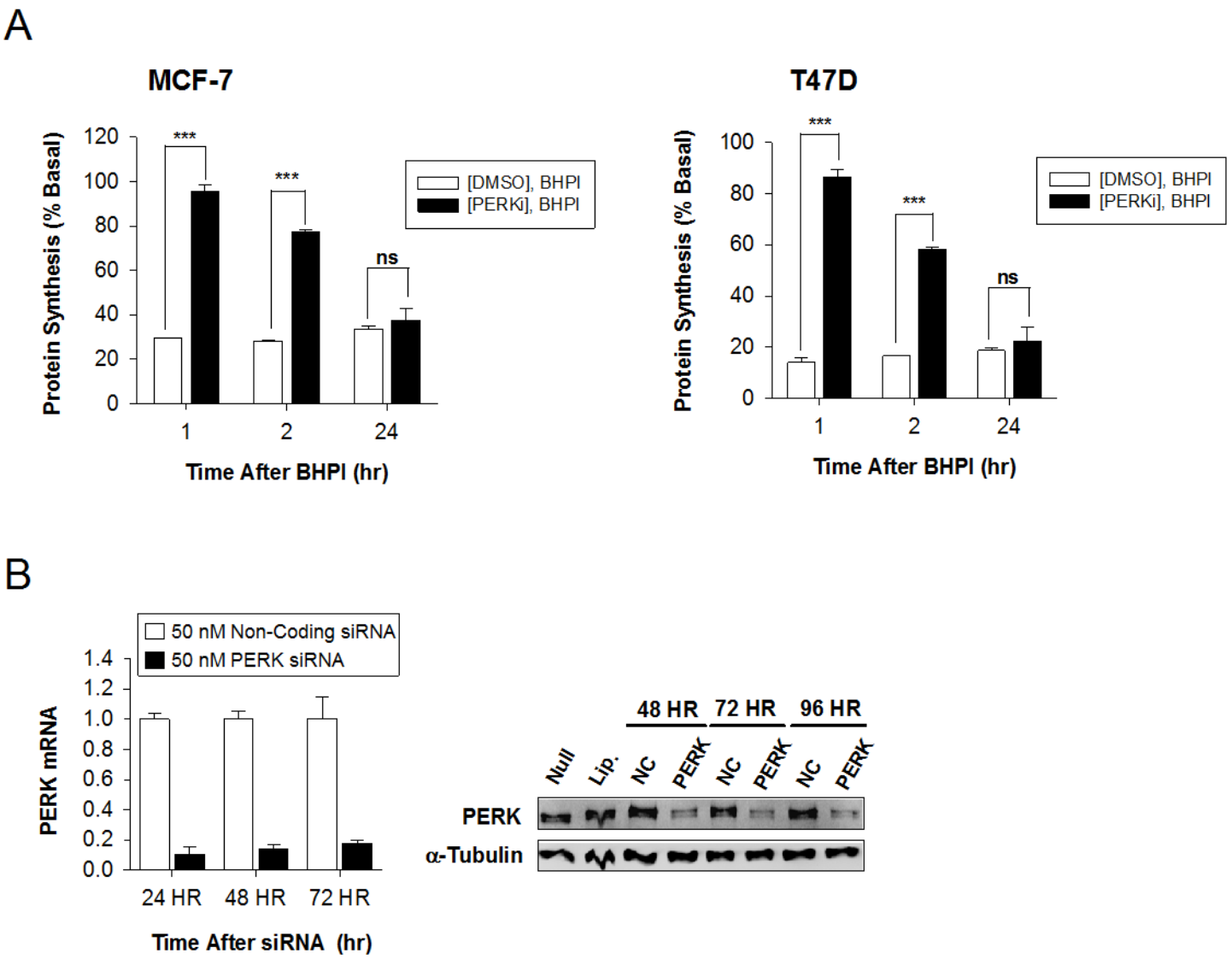

Fig. S9. Blocking PERK activation or PERK knockdown largely blocks inhibition of protein synthesis at early times after BHPI treatment, but does not prevent BHPI from inhibiting protein synthesis at later times. (*A*) Inhibiting PERK activation with the PERK inhibitor, GSK2606414 (PERKi) (14, 15), blocks rapid BHPI inhibition of protein synthesis in MCF-7 and T47D cells (n = 4). Cells were pre-treated for 1 hour with DMSO-vehicle or 1 μM GSK2606414, followed by treatment with 100 nM BHPI for the indicated times. (*B*) RNAi knockdown of PERK mRNA and protein. MCF-7 cells were transfected with either 50 nM PERK siRNA SmartPool (PERK) or with 50 nM of a control non-coding SmartPool (NC). PERK mRNA levels were determined by qRT-PCR with 36B4 as internal standard. Set to 1 at each time was the level of PERK mRNA in cells transfected with the Non-coding control (NC) siRNA. Shown is a Western blot of PERK protein levels after transfection with PERK siRNA and control siRNA (NC). Null: control cells, no transfection; Lip: liposome only no siRNA. Data is the mean ± SEM. *** $p < 0.001$; ns, not significant ($p > 0.05$).

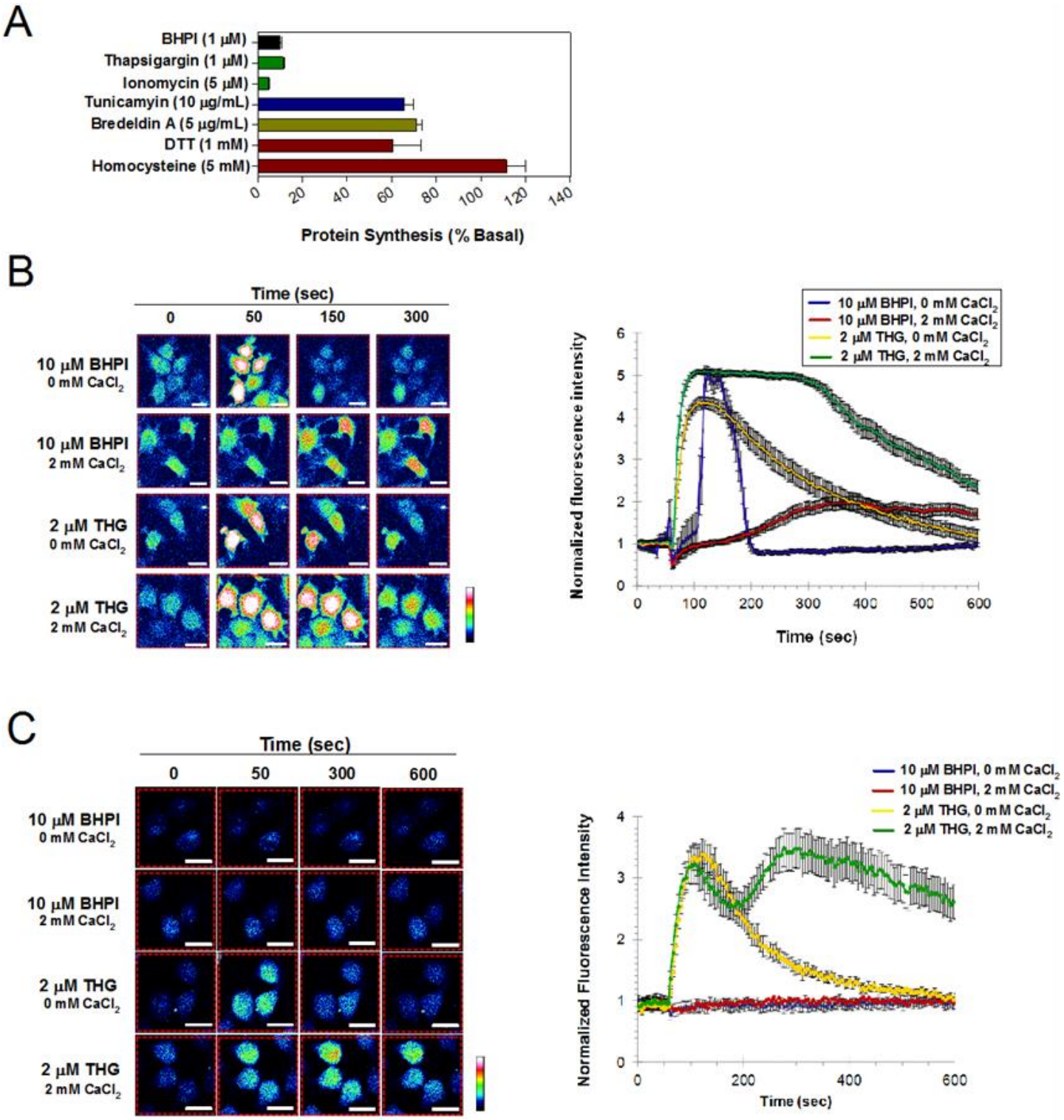

Fig. S10. BHPI activates the UPR through depletion of endoplasmic reticulum calcium stores in ERα$^+$ MCF-7 breast cancer cells, but not in ERα$^-$ HeLa cervical cancer cells. (*A*) Protein synthesis in MCF-7 cells treated for 2 hours with UPR activators (n = 6). Effect of BHPI and Thapsigargin (THG) on intracellular calcium levels in (*B*) ERα$^+$ MCF-7 breast cancer cells and (*C*) ERα$^-$ HeLa cervical cells. Although BHPI has no effect, HeLa cells remain sensitive to Thapsigargin. Cells visualized with the Ca^{2+} sensitive dye Fluo-4 AM. Low levels of basal [Ca^{2+}] are blue and then green, whereas higher levels of [Ca^{2+}] are seen as red, with the highest levels white.

Trace represents calcium following treatment with Thapsigargin or BHPI. Intensity was normalized to the basal signal, which was set to 1. Data is mean ± SEM (n = 10).

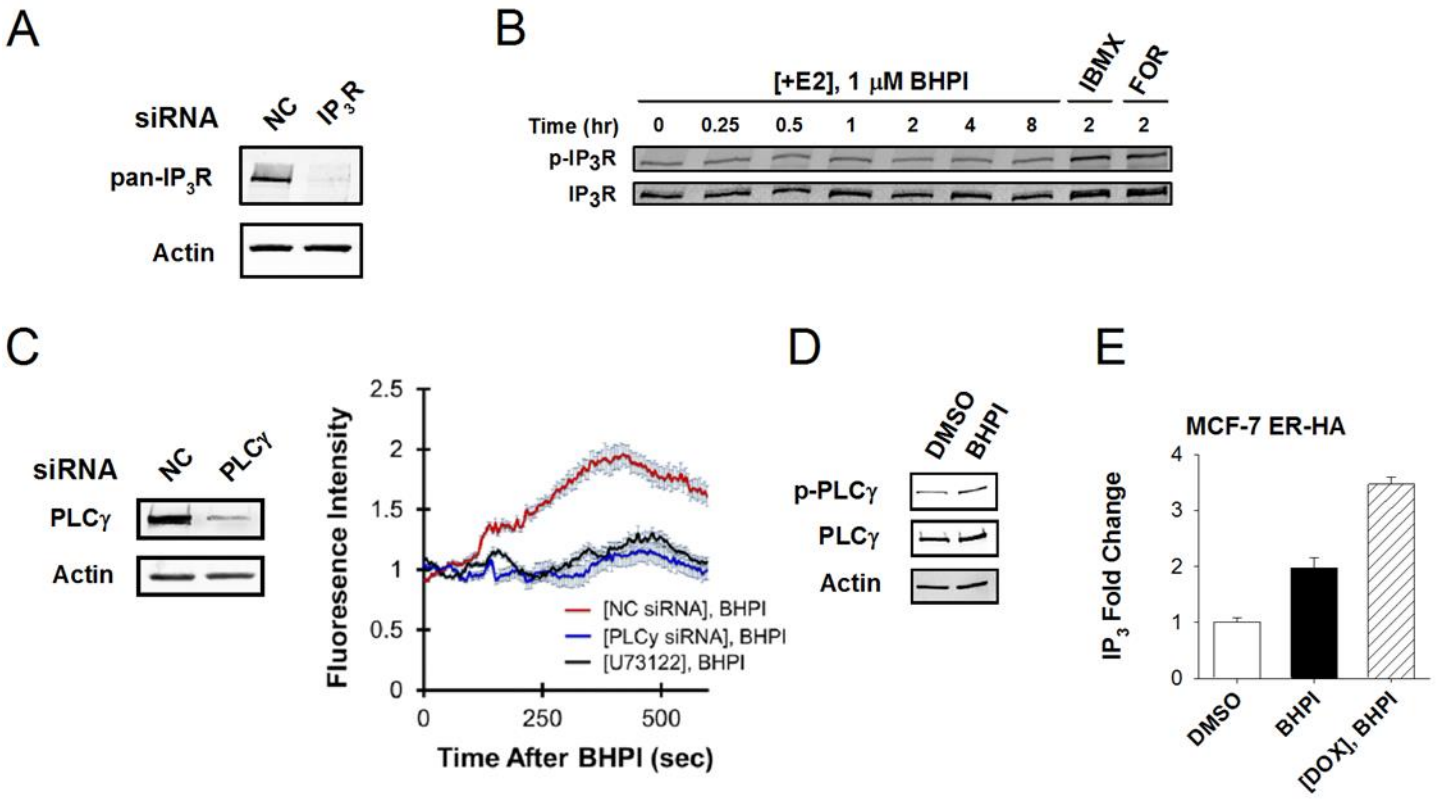

Fig. S11. Effects of BHPI on IP_3R, IP_3, and PLCγ. (*A*) Western blot analysis of pan-IP_3R protein levels after treatment of MCF-7 cells with either 100 nM non-coding (NC) SmartPool siRNA or 100 nM SmartPool IP_3R siRNA. Data in panel *A* is from ([4], supplementary figures). (*B*) Time course of phosphorylation of the IP_3R Ca^{2+}-channel and total IP_3R following treatment with BHPI. Phosphorylation of IP_3R at Ser-1756 by cyclic AMP-dependent protein kinase A (PKA) regulates the activity of the IP_3R Ca^{2+}-channel. While BHPI had no effect, the MCF-7 cells contain a functional protein kinase A pathway since the protein kinase A activators, IBMX and Forskolin, increased phosphorylation of IP_3R. (*C*) Effects of BHPI on cytosol Ca^{2+} following either PLCγ knockdown or blocking PLCγ activation with U73122. Western blot shows PLCγ protein levels following treatment of MCF-7 cells with either 100 nM non-coding SmartPool siRNA or 100 nM SmartPool PLCγ siRNA. (*D*) Effects of BHPI on phosphorylation and activation of PLCγ. Phosphorylation of PLCγ at Tyr-1756 regulates the activity of PLCγ. MCF-7 cells were treated for 10 min. with 1 μM BHPI. (*E*) Effects of overexpressing ERα on BHPI-induced increases in IP_3 levels. ERα in MCF7ERαHA cells was induced with DOX as described in Figure 3*E*. IP_3 levels were determined 10 min. after treatment with 1 μM BHPI. Data is mean ± SEM (n=3).

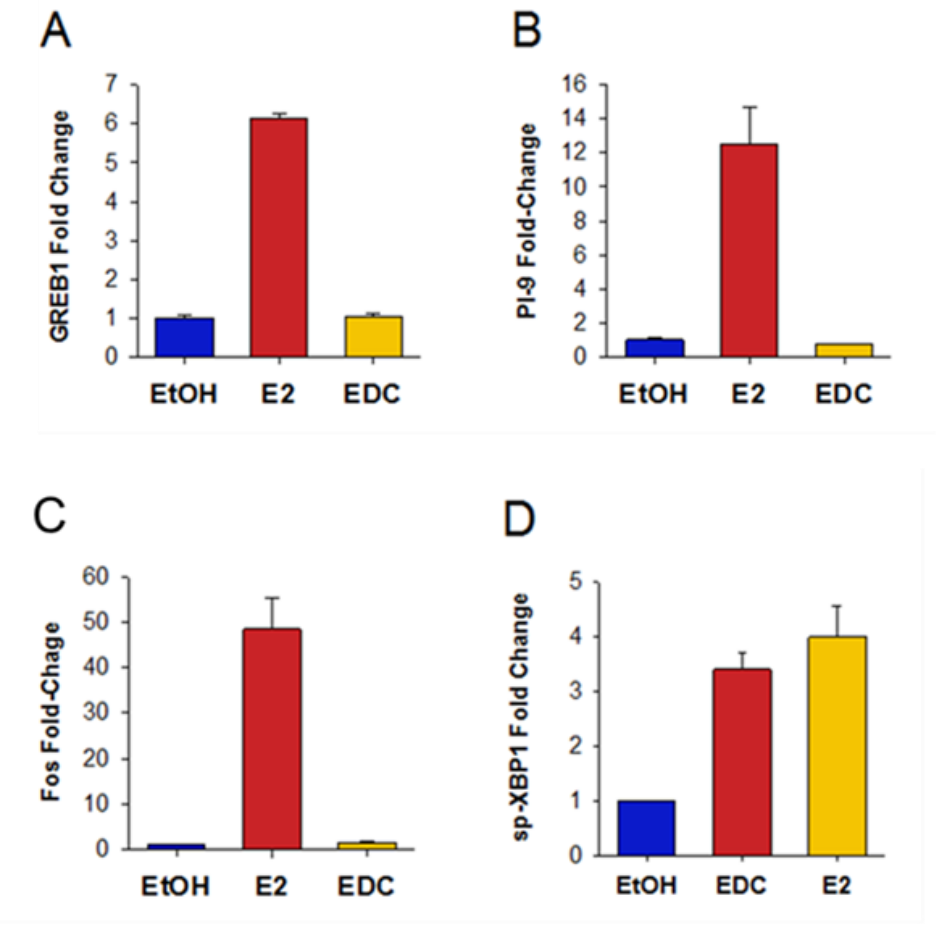

Figure S12. Comparison of effects of 17β-estradiol (E2) and estrogen-dendrimer-conjugate (EDC) on the ability of ERα to activate (*A*) GREB1, (*B*) PI-9, and (*C*) Fos expression. These are classical estrogen-regulated genes. (*D*) Comparison of the effects of E2 and EDC on the ability to induce spliced-XBP1 (sp-XBP1), which is a widely used marker of UPR activation (see UPR model in Figure S7*C*).

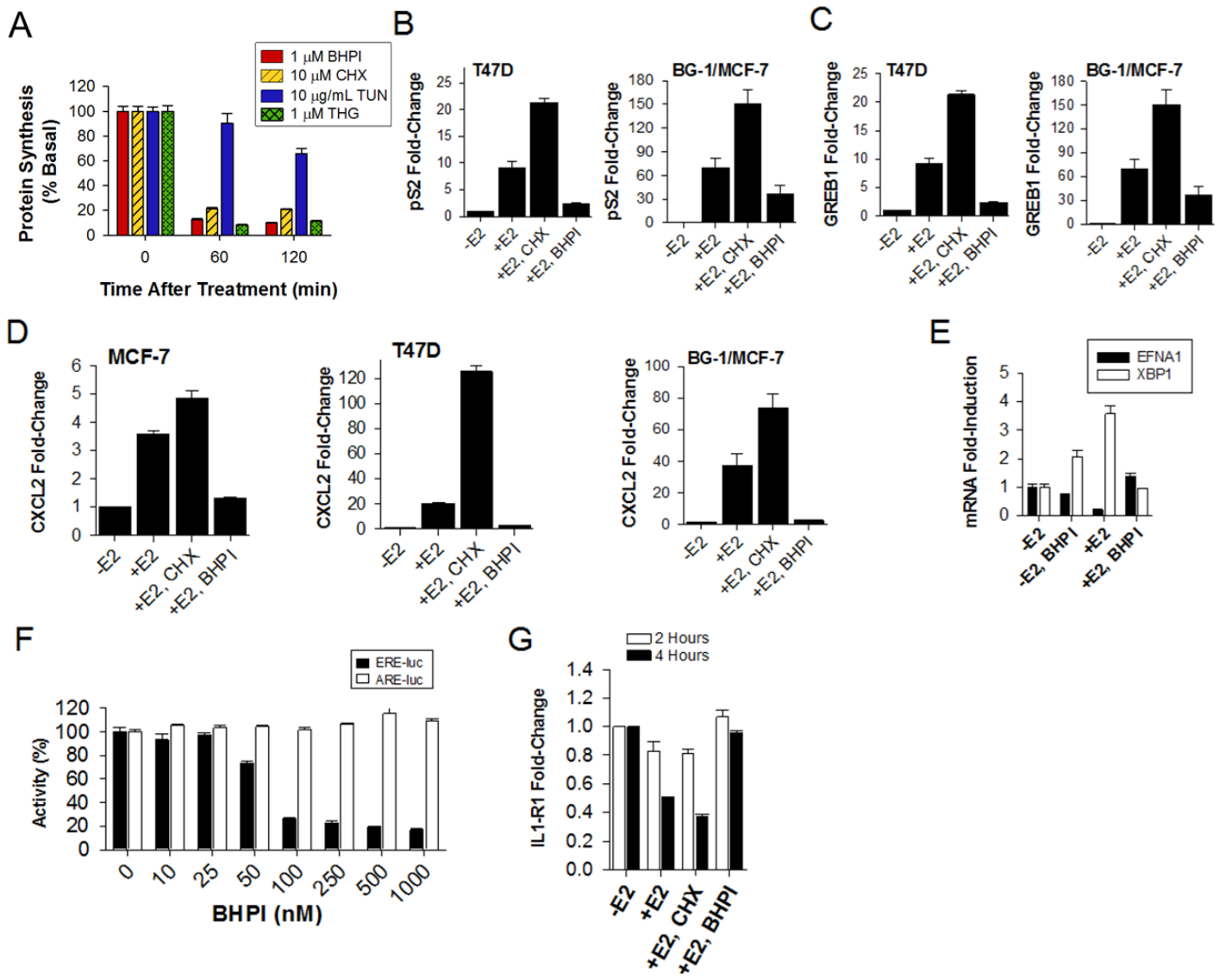

Fig. S13. BHPI inhibits E_2-ERα regulated gene expression. (*A*) Comparison of the effects of BHPI, the protein synthesis inhibitor cycloheximide (CHX), and the UPR activators Tunicamycin (TUN) or thapsigargin (THG) on protein synthesis. Since protein synthesis was robustly inhibited by CHX after 120 minutes, this time was used in the gene expression studies. Effects of BHPI on E_2-ERα induction of (*B*) pS2, (*C*) GREB1 and (*D*) CXL2 mRNAs and (*E*) XBP1 in MCF-7, T47D and BG-1/MCF-7 cells. Cells were pretreated with either 1 μM BHPI (+E2, BHPI), 10 μM cycloheximide (+E2, CHX), or 0.1% DMSO (+E2; -E2) for 30 minutes, followed by treatment with either 10 nM E_2 (+E2; +E2, BHPI; +E2, CHX) or 0.1% ethanol-vehicle control (-E2) for 2 hours. (*F*) Dose response studies of the effect of BHPI on E_2-ERα induction of ERE-luciferase activity in ERα positive T47D-kBluc breast cancer cells (black bars) and for dihydrotestosterone-androgen receptor (DHT-AR) induction of prostate specific antigen (PSA)-luciferase in ERα negative HeLaA6 cells (open bars). HeLaA6 cells are stably transfected to express AR and a PSA-luciferase reporter. Supporting specificity of BHPI, it did not inhibit DHT-AR induction of ARE-luciferase. BHPI blocks E_2-ERα down-regulation of EFNA1 in MCF-7 cells (*E*) and IL1-R1 in T47D cells (*G*). Data is mean ± SEM (n = 3).

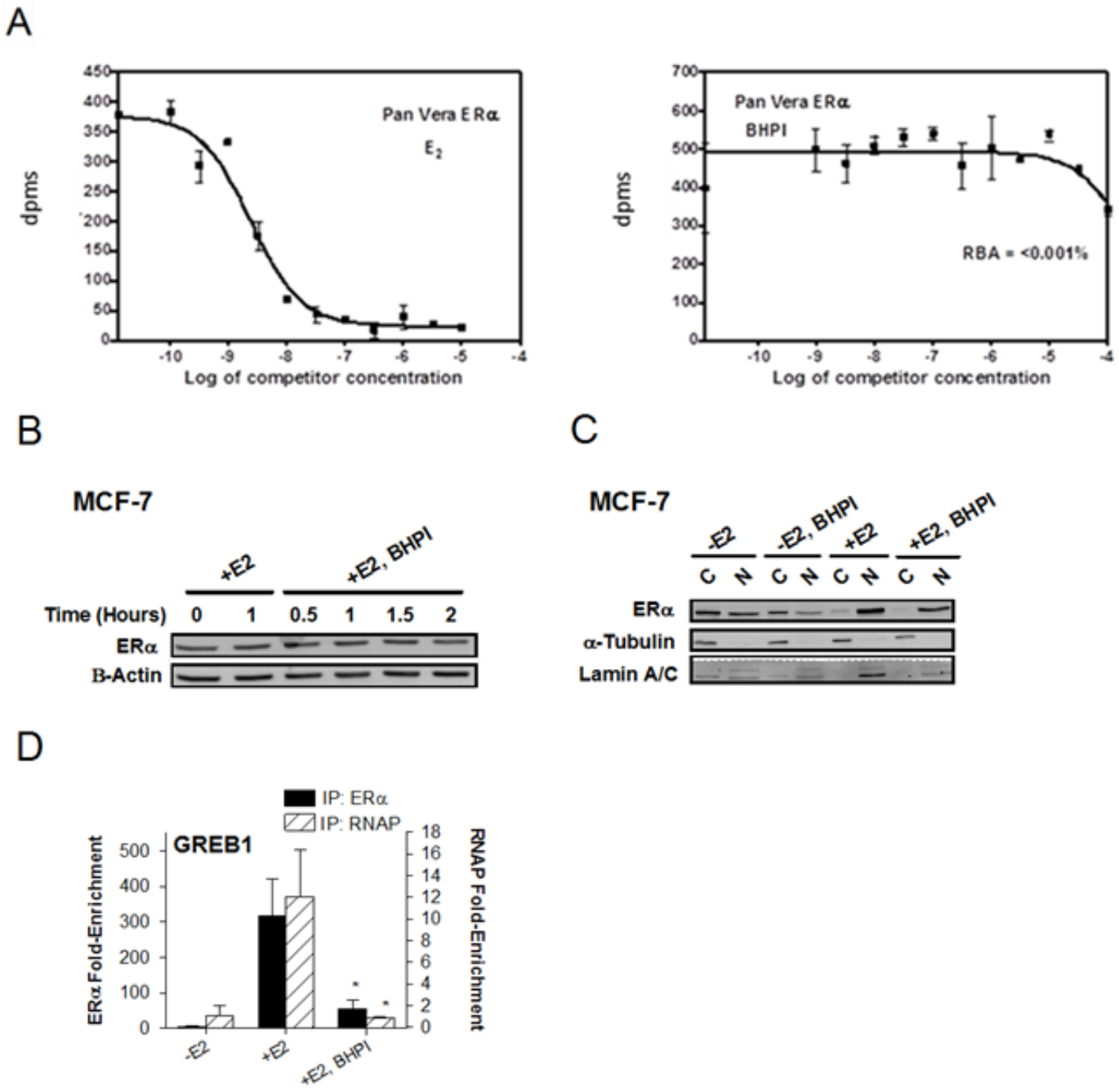

Fig. S14. BHPI is a non-competitive inhibitor that reduces binding of E_2-ERα to gene regulatory regions. BHPI does not compete with estrogens for binding to ERα. (*A*) Competitive radioligand binding assay comparing the ability of E_2 and BHPI to compete with [^{3}H] estradiol (E_2) for binding to ERα. The relative binding affinity (RBA) of BHPI for the estrogen-binding pocket of ERα was determined using 0.2 nM [^{3}H] E_2 and a range of BHPI concentrations. RBA values were determined from the competitive radiometric binding assay (7, 16). Values are expressed as percentages relative to the affinity of the standard, E_2 = 100%. (*B*) Western blots showing that at early times after treatment with 1 μM BHPI, ERα protein levels are nearly unchanged. (*C*) Western blot showing that treatment of MCF-7 cells with 1 μM BHPI does not inhibit nuclear localization of ERα. α-Tubulin and lamin A/C were controls for the cytoplasmic and nuclear fractions, respectively. ERα protein levels and nuclear localization were assessed 2 hours after treatment, which was the same time used to assess endogenous mRNA levels of E_2-ERα regulated genes via qRT-PCR. (*D*) ChIP shows that 1 μM BHPI BHPI inhibits recruitment of E_2-ERα (black bars) and RNA polymerase II (RNAP, hatched bars) to the GREB1 promoter region. Data is mean ± SEM (n = 3). * Significant at ($p < 0.05$).

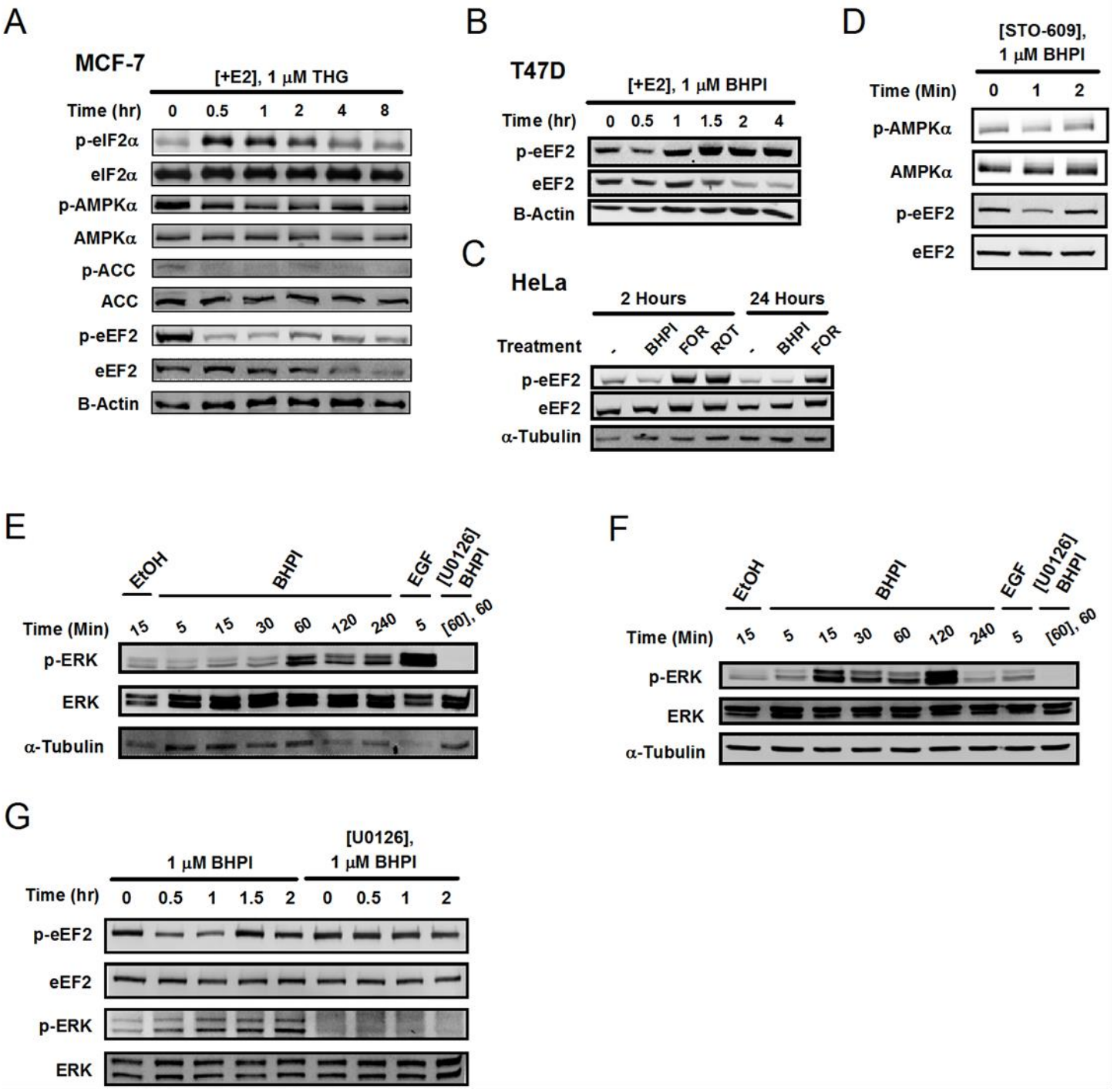

Fig. S15. Conventional UPR activators do not induce phosphorylation of eEF2, but induces transient eIF2α phosphorylation, transient inhibition of protein synthesis, and induction of chaperones. (*A*) Analysis of the time course of Thapsigargin (THG) effects on phosphorylation of eIF2α (Ser-51), AMPKα (Thr-172), ACC (Ser-79), and eEF2 (Thr-56). Unlike BHPI, Thapisgargin does not induce phosphorylation of eEF2 but induces transient phosphorylation of eIF2α. Western blots of the time course of BHPI effects on phosphorylation of eEF2 (Thr-56) in (*B*) ERα positive T47D and (*C*) ERα negative HeLa cells. T47D Cells were pre-treated with 10 nM E2 for 24-hours. eEF2 is essential for protein synthesis, and eEF2-Ser^{56} phosphorylation inactivates eEF2, blocking the elongation step of protein synthesis. The positive controls, Forskolin (FOR) and Rottlerin (ROT) induce robust eEF2 phosphorylation, demonstrating eEF2 retains the capacity for phosphorylation in HeLa cells. (*D*) Inhibiting AMPK phosphorylation and activation with ST-609 did not block BHPI-stimulated phosphorylation of

eEF2. Effects of BHPI on Thr-202/Thr-204 phosphorylation of p44/p42 MAPK (p-ERK) in ERα positive (*E*) MCF-7 cells and (*F*) T47D cells. Activation of p44/p42 MAPK promotes the phosphorylation and inactivation of eEF2K. The classical ERK activator, EGF (20 ng/ml), served as a positive control for ERK1/2 phosphorylation. As a control, cells were treated with 10 μM UO126 for the indicated times. U0126 inhibits the upstream kinase MEK1/2, inhibiting ERK1/2 phosphorylation. UO126 pre-treatment was for 2 hours. (*G*) Effects of blocking ERK activation with U0126 on BHPI-induced phosphorylation of eEF2. By inhibiting the ERK pathway, UO126 allows eEF2K to be active and the reduced activation seen at 0.5 and 1 hours due to BHPI-induced ERK activation is abolished.

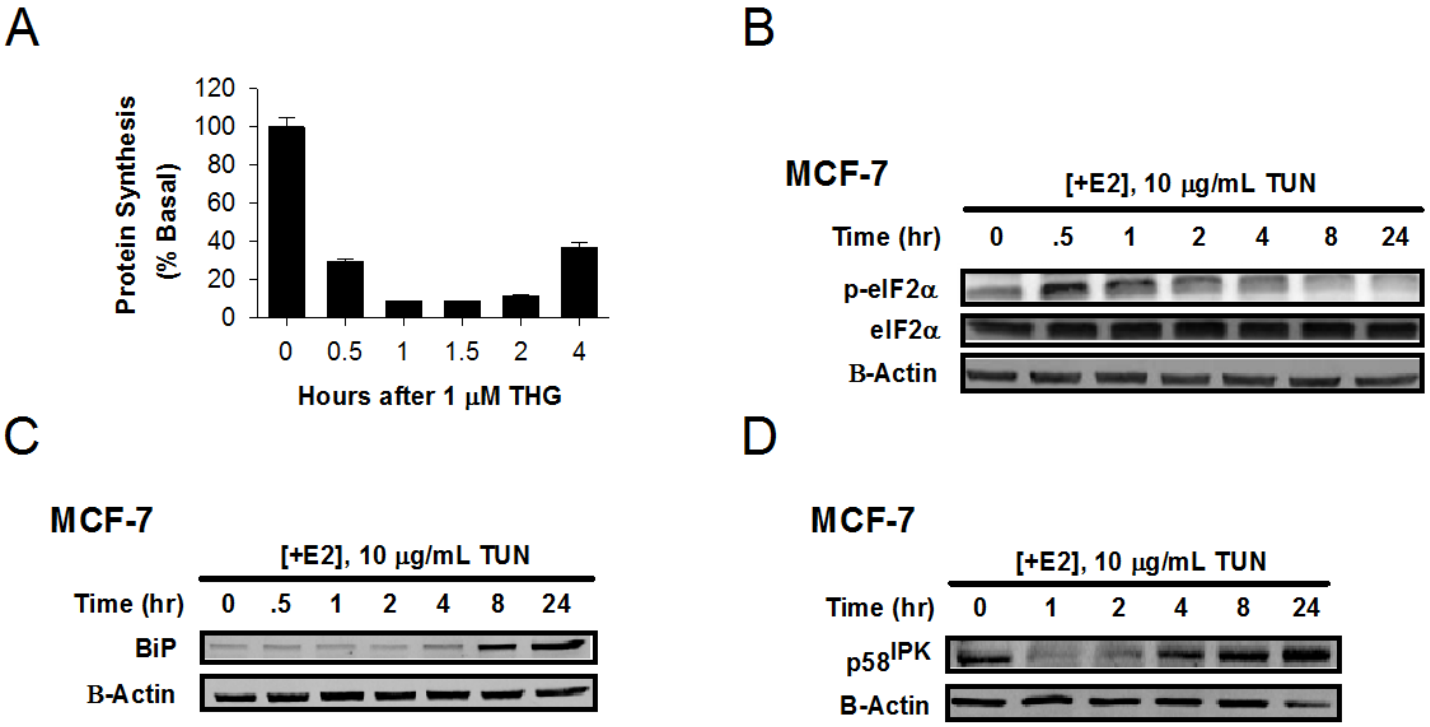

Fig. S16. The UPR activators, Thapsigargin and Tunicamycin, reversibly activate the UPR. Induction of BiP and p58^{IPK} normally helps resolve UPR stress and reverses UPR activation. (*A*) Time course of THG inhibition of protein synthesis. Consistent with transient phosphorylation of eIF2α by THG (see Fig. S15*A*) and resolution of UPR stress, protein synthesis begins to recover at 4 hours after treatment with THG. (*B*) Western blot analysis of phosphorylation of eIF2α following TUN treatment. TUN induces transient phosphorylation of eIF2α. Western blot analysis showing the time course of Tunicamycin (TUN) induction of BiP (*C*) and p58^{IPK} (*D*) in MCF-7 cells. Data in panel *C* is from ([4], supplementary figures). Data is mean ± SEM (n = 3). (*A-D*) 24-hour pre-treatment with 10 nM E_2.

SI References

1. Putt KS & Hergenrother PJ (2004) A nonradiometric, high-throughput assay for poly(ADP-ribose) glycohydrolase (PARG): application to inhibitor identification and evaluation. *Anal Biochem* 333(2):256-264.
2. Andruska N, Mao C, Cherian M, Zhang C, & Shapiro DJ (2012) Evaluation of a luciferase-based reporter assay as a screen for inhibitors of estrogen-ERalpha-induced proliferation of breast cancer cells. *J Biomol Screen* 17(7):921-932.
3. Cherian MT, Wilson EM, & Shapiro DJ (2012) A competitive inhibitor that reduces recruitment of androgen receptor to androgen-responsive genes. *J Biol Chem* 287(28):23368-23380.
4. Andruska N, Zheng X, Yang X, Helferich WG, & Shapiro DJ (2014) Anticipatory estrogen activation of the unfolded protein response is linked to cell proliferation and poor survival in estrogen receptor α-positive breast cancer. *Oncogene* 33(advance online publication, September 29, 2013).
5. Kretzer NM*, et al.* (2010) A noncompetitive small molecule inhibitor of estrogen-regulated gene expression and breast cancer cell growth that enhances proteasome-dependent degradation of estrogen receptor {alpha}. *J Biol Chem* 285(53):41863-41873.
6. Cheng J, Zhang C, & Shapiro DJ (2007) A functional serine 118 phosphorylation site in estrogen receptor-alpha is required for down-regulation of gene expression by 17beta-estradiol and 4-hydroxytamoxifen. *Endocrinology* 148(10):4634-4641.
7. Carlson KE, Choi I, Gee A, Katzenellenbogen BS, & Katzenellenbogen JA (1997) Altered ligand binding properties and enhanced stability of a constitutively active estrogen receptor: evidence that an open pocket conformation is required for ligand interaction. *Biochemistry* 36(48):14897-14905.
8. Ju YH, Doerge DR, Allred KF, Allred CD, & Helferich WG (2002) Dietary genistein negates the inhibitory effect of tamoxifen on growth of estrogen-dependent human breast cancer (MCF-7) cells implanted in athymic mice. *Cancer Res* 62(9):2474-2477.
9. Harrington WR*, et al.* (2006) Estrogen dendrimer conjugates that preferentially activate extranuclear, nongenomic versus genomic pathways of estrogen action. *Mol Endocrinol* 20(3):491-502.
10. Ron D & Walter P (2007) Signal integration in the endoplasmic reticulum unfolded protein response. *Nat Rev Mol Cell Biol* 8(7):519-529.
11. Walter P & Ron D (2012) The unfolded protein response: from stress pathway to homeostatic regulation. *Science* 334(6059):1081-1086.
12. Wu J*, et al.* (2007) ATF6alpha optimizes long-term endoplasmic reticulum function to protect cells from chronic stress. *Dev Cell* 13(3):351-364.
13. Hetz C, Martinon F, Rodriguez D, & Glimcher LH (2011) The unfolded protein response: integrating stress signals through the stress sensor IRE1alpha. *Physiol Rev* 91(4):1219-1243.
14. Axten JM*, et al.* (2012) Discovery of 7-methyl-5-(1-{[3-(trifluoromethyl)phenyl]acetyl}-2,3-dihydro-1H-indol-5-yl)-7H-p yrrolo[2,3-d]pyrimidin-4-amine (GSK2606414), a potent and selective first-in-class inhibitor of protein kinase R (PKR)-like endoplasmic reticulum kinase (PERK). *J Med Chem* 55(16):7193-7207.
15. Harding HP, Zyryanova AF, & Ron D (2012) Uncoupling proteostasis and development in vitro with a small molecule inhibitor of the pancreatic endoplasmic reticulum kinase, PERK. *J Biol Chem* 287(53):44338-44344.
16. Katzenellenbogen JA, Johnson HJ, Jr., & Myers HN (1973) Photoaffinity labels for estrogen binding proteins of rat uterus. *Biochemistry* 12(21):4085-4092.